ECCOMAS Congress 2016
VII European Congress on Computational Methods in Applied Sciences and Engineering
M. Papadrakakis, V. Papadopoulos, G. Stefanou, V. Plevris (eds.)
Crete Island, Greece, 5–10 June 2016

A LEAST-SQUARES, ADAPTIVE UNCERTAINTY PROPAGATION APPROACH FOR A PLASMA-COUPLED COMBUSTION SYSTEM

Kunkun Tang, Luca Massa, Jonathan Wang and Jonathan B. Freund

The Center for Exascale Simulation of Plasma-coupled Combustion (XPACC)
University of Illinois at Urbana-Champaign
1308 W Main St, Urbana IL 61801, USA
e-mail: {ktg,luca1,jmwang2,jbfreund}@illinois.edu

Keywords: Uncertainty quantification, Sensitivity analysis, Adaptive ANOVA, Polynomial dimensional decomposition (PDD), Combustion.

Abstract. *We employ a new stochastic methodology for the construction of surrogate models for uncertainty quantification (UQ) and sensitivity analysis (SA). It is based on polynomial dimensional decomposition (PDD), as are widely used in solving high-dimensional stochastic problems that arise in various applications. In our approach, the coefficients of the PDD expansion are determined by using a least-squares regression (LSR). Compared to a projection approach, the use of LSR not only avoids the computation of high-dimensional integrals, but also affords an attractive flexibility in choosing the sampling points, which facilitates importance sampling using a calibrated posterior distribution based on a Bayesian approach. LSR can be particularly advantageous in cases where the asymptotic convergence properties of polynomial expansions cannot be realized due to computation expense, focusing effort on efficient finite-resolution sampling. To efficiently include parameter spaces with a moderate number of uncertain parameters (up to 7 in this work), the PDD is coupled with an adaptive ANOVA (analysis of variance) decomposition. This provides an accurate surrogate as the union of several low-dimensional spaces, avoiding the typical computational overhead cost of a high-dimensional expansion. In addition, the PDD representation of the ANOVA component functions is further simplified in an adaptive way according to the relative contribution of the different polynomials to the variance. The overall methodology is demonstrated on plasma-mediated ignition simulations as part of a large predictive science effort in the Center for Exascale Simulation of Plasma-Coupled Combustion (XPACC). The specific configuration we study includes model parameters arising from reaction rates in a global chemical kinetics description, and a laser-induced breakdown ignition seed.*

1 INTRODUCTION

It is well-understood that global sensitivity analysis (GSA) has the advantage of taking into account the broad influence of input parameters over the ranges and their interactions onto the output quantity of interest, by considering the entire input space rather than a specific nominal point (see for example [6]). However, the main difficulty encountered when employing global methods is the high cost of Monte Carlo (MC) or a quasi Monte Carlo (QMC) methods. These can be prohibitively expensive.

The objective of this work consists of building an efficient Uncertainty Quantification (UQ) and GSA method featuring a surrogate model representation that is affordable for complex numerical simulation problems. To address the so-called curse of dimensionality, we employ the polynomial dimensional decomposition (PDD) (introduced and developed by Rahman and coworkers in e.g. [12, 13, 15, 21, 14]) and combine it with the Analysis of Variance (ANOVA) decomposition due to their direct link with each other. The least-squares regression (LSR) approach is an efficient tool to determine the expansion coefficients, by minimizing the error of the surrogate model representation in the mean square sense (see e.g. [7, 18, 3]). Compared to the projection approach (see e.g. [9, 11, 2]) where each polynomial coefficient is obtained by computing a multi-dimensional integral, the regression approach is more flexible (in choosing sampling points) for problems involving a moderate number of uncertain parameters. It is known that the number of ANOVA component functions increases exponentially with respect to the uncertain parameter dimensionality, and meanwhile the imposed polynomial order for the PDD expansion involves a polynomial increase of the number of PDD terms for each component function. This phenomenon causes one main limitation of the regression approach even for a truncated low-order ANOVA expansion, namely the high number of deterministic model evaluations for problems characterized by a moderate to large number of uncertainties; indeed, for the regression problem to be well posed, the number of deterministic model evaluations is necessary to be larger than the total polynomial expansion size [3, 4]. In this respect, this paper employs the approach proposed in [20] to combine the *active dimension* strategy and the *stepwise regression* technique [3, 4] to obtain an efficient sparse surrogate model representation.

In Section 2, we review basic concepts of ANOVA, Sobol' sensitivity indices and outline main idea of variance-based dimension reduction techniques. A 2-D axisymmetric application case is investigated in Section 3. Conclusions follow.

2 ANOVA AND VARIANCE-BASED DIMENSION REDUCTION

Let us suppose that the response of a given system of interest can be represented by a N-dimensional function $y = f(\boldsymbol{\xi})$

$$y = f(\boldsymbol{\xi}) = f(\xi_1, \xi_2, \cdots, \xi_N), \tag{1}$$

where $\boldsymbol{\xi}$ are independent input uncertain parameters.

An Analysis of Variance (ANOVA) [16, 8, 1, 17] decomposes $f(\boldsymbol{\xi})$ into a series of lower-dimentional component functions as

$$y = f_0 + \sum_{1 \leqslant i \leqslant N}^{N} f_i(\xi_i) + \sum_{1 \leqslant i < j \leqslant N}^{N} f_{ij}(\xi_i, \xi_j) + \cdots + f_{1,2,\cdots,N}(\xi_1, \xi_2, \cdots, \xi_N), \tag{2}$$

or in compact form

$$y = f_0 + \sum_{T=1}^{N} \sum_{i_1<\cdots<i_T}^{N} f_{i_1,\cdots,i_T}(\xi_{i_1}, \cdots, \xi_{i_T}). \tag{3}$$

Note in ANOVA component functions have zero mean and are orthogonal. For notational convenience in this section, we write a general T-dimensional component function ($1 \leq T \leq N$) of the ANOVA decomposition as

$$f_{\mathbf{i}_T}(\boldsymbol{\xi}_T) = f_{i_1,i_2,\cdots,i_T}(\xi_{i_1}, \xi_{i_2}, \cdots, \xi_{i_T}). \tag{4}$$

Keeping in mind its zero-mean property, the component function (4) can be expanded by employing Polynomial Dimensional Decomposition (PDD) using an infinite number of orthogonal basis functions (as done in [12]) by a tensor product for multi-indices $\mathbf{j}_T$:

$$f_{\mathbf{i}_T}(\boldsymbol{\xi}_T) = \sum_{j_T,\cdots,j_1}^{\infty} C_{\mathbf{i}_T}^{\mathbf{j}_T} \Psi_{\mathbf{i}_T}^{\mathbf{j}_T}. \tag{5}$$

Here $C_{\mathbf{i}_T}^{\mathbf{j}_T}$ is a coefficient, and $\Psi_{\mathbf{i}_T}^{\mathbf{j}_T}$ is a T-dimensional basis polynomial function.

In practice, the expansion with an infinite number of terms in (5) must be truncated. Following previous work [12], we truncate (5) by m terms for each dimension:

$$f_{\mathbf{i}_T}(\boldsymbol{\xi}_T) = \sum_{j_T,\cdots,j_1 \leq m} C_{\mathbf{i}_T}^{\mathbf{j}_T} \Psi_{\mathbf{i}_T}^{\mathbf{j}_T}. \tag{6}$$

In particular, the first-order, second-order, and third-order component functions are expressed as

$$\begin{aligned} f_i(\xi_i) &= \sum_{j=1}^{m} C_i^j \psi^j(\xi_i), \\ f_{\mathbf{i}_2}(\boldsymbol{\xi}_{\mathbf{i}_2}) &= \sum_{j_2=1}^{m} \sum_{j_1=1}^{m} C_{\mathbf{i}_2}^{\mathbf{j}_2} \psi^{j_1}(\xi_{i_1}) \psi^{j_2}(\xi_{i_2}), \\ f_{\mathbf{i}_3}(\boldsymbol{\xi}_{\mathbf{i}_3}) &= \sum_{j_3=1}^{m} \sum_{j_2=1}^{m} \sum_{j_1=1}^{m} C_{\mathbf{i}_3}^{\mathbf{j}_3} \psi^{j_1}(\xi_{i_1}) \psi^{j_2}(\xi_{i_2}) \psi^{j_3}(\xi_{i_3}). \end{aligned} \tag{7}$$

Least-squares regression (LSR) [5, 20] can be employed to determine the coefficients $\mathbf{C}_\alpha$ of (vector-form) PDD expansion

$$f(\boldsymbol{\xi}) = \mathbf{C}_\alpha^T \Phi_\alpha(\boldsymbol{\xi})$$

by using a suitable set of training points (i.e. experimental design) and model outputs. The second-order moment and the global sensitivity indices can be obtained in a straightforward way by post-processing.

Indeed, keeping in mind

$$E(f(\boldsymbol{\xi})) = C_{\alpha_0},$$

the approximated variance of the model output is then

$$\mathrm{Var}(f(\boldsymbol{\xi})) = \sum_{j=1}^{P-1} C_{\alpha_j}^2 \gamma_{\alpha_j},$$

with the multivariate normalization constant determined by

$$\gamma_{\alpha_j} = E\left[\Phi^2_{\alpha_j}(\boldsymbol{\xi})\right],$$

where P is the expansion size.

It is straightforward to write the variance-based global sensitivity indices (SI) by using the PDD expansion. Indeed,

$$\mathcal{S}_{i_1,\cdots,i_T} = \frac{\mathrm{Var}(f_{i_1,\cdots,i_T})}{\mathrm{Var}(f(\boldsymbol{\xi}))} = \frac{1}{\mathrm{Var}(f(\boldsymbol{\xi}))} \sum_{\alpha_j \subseteq (i_1,\cdots,i_T)} C^2_{\alpha_j} \gamma_{\alpha_j}. \tag{8}$$

The total sensitivity index $\mathcal{S}_i^T$ can be obtained simply by adding all the measures $\mathcal{S}_{i_1,\cdots,i_T}$ whose index involves the variable ξ_i.

For practical problems, in particular for the ones with a large number of stochastic parameters, the size of the PDD representation must be reduced to make the uncertainty analysis feasible.

A stepwise regression method has been proposed in [4, 3] using a generalized Polynomial Chaos (gPC) approach to build sparse polynomial representation of the model output. In order to efficiently represent a moderate to large dimensional parameter space, in addition to the stepwise regression technique proposed in [4, 3], the PDD approach used in this work is further coupled with an adaptive ANOVA decomposition, which allows to model a given number of low-dimensional spaces instead of a single high-dimensional one. The overall adaptive technique, as a variant of the one used in [4, 3], has been proposed in [20]. We summarize this LSR strategy as a set of coupled adaptive strategies as follows.

1. Set a truncation dimension ν (the maximum interaction order) in the ANOVA expansion. This follows the assumption that low-order interactions are of dominant importance compared to their high-order counterparts.

2. Solve the LSR system including only the PDD terms of the first-order ANOVA component functions, and a rank of importances can then be established quantitatively for all the input parameters. Hence, we retain only so-called active dimensions (the most influential parameters) for the PDD terms of the second- and higher-order ANOVA components. Let us use D_T to represent the active dimension for interaction order T.

3. Enrich the surrogate model representation by adding one-by-one significant polynomials of second- and higher-order interaction terms by keeping only the corresponding active dimensions. A variance-based selection criterion is used to retain only polynomials of significant importance to the total variance, which allows to build a very sparse model representation. We emphasize that recursive resolutions of regression problems are required for this task.

In next section, this adaptive LSR ANOVA approach is applied to an application case featuring input uncertainties arising from chemical kinetics and laser-induced breakdown ignition seed.

3 APPLICATION TO A 2-D COMBUSTION SYSTEM

The combustion in this work is modeled by multi-species Navier–Stokes equations involving source terms including contributions from a reduced chemical mechanism, and

a simplified laser-induced breakdown (LIB) plasma model. Both thermal and vortical contributions are modeled for LIB ignition seed [10]. The model parameter uncertainties considered in this work mainly come from these source terms.

Note the system of Navier–Stokes equations is discretized by finite difference methods on structured grids using the software *PlasComCM*. For details on numerical techniques, we refer to [10].

3.1 Source of uncertainties

The present combustion model featuring a Laser Induced Breakdown (LIB) ignition seed includes seven uncertain parameters, which are calibrated against low-dimensional computations or estimated based on experiments or previous literature data. We summarize these uncertain parameters in Table 1. Note A_3, b_3, and E_3 are calibrated Arrhenius

Combustion kinetics	A_3	Joint pdf_{post} calibrated	
	b_3		
	E_3		
Laser Induced Breakdown	$L_{TW} \sim \mathcal{U}(0.993, 2.979)$		[mm]
	$R_{TW}(= D_{TW}/2) \sim \mathcal{U}(0.168, 0.504)$		[mm]
	$M_e \sim \mathcal{U}(1, 3)$		
	$E_{abs} \sim \mathcal{N}(17.642, 3.1157)$		[mJ]

Table 1: Summary of uncertain model parameters.

coefficients of the following reaction,

$$2H_2 + O_2 + H \rightarrow 2H_2O + H. \tag{9}$$

L_{TW} (resp. R_{TW}) represents the length (resp. radius) of the luminosity region measured by experiments (we assume the laser energy is spatially distributed over the luminosity region). M_e is the Mach number of LIB vorticity model, and finally, E_{abs} is the absorbed laser energy. The reader is refered to [10] for detailed physical modeling of LIB. Among the four parameters of LIB, the Gaussian distribution of E_{abs} is approximated using experimental results (3160 trials). However, we know significantly less about other three parameters. Thus, L_{TW} and R_{TW} are simply taken to follow a uniform distribution using an error bar of 50 % of their norminal value. The upper-bound value of $M_e = 3$ is the threshold with which our current numerical model becomes significantly unstable.

3.2 Axisymmetric 2-D test problem and quantity of interest (QoI)

An ignition case is computed on a 2-D rectangular domain (as shown in Fig. 1) discretized as a structured grid of size 501×503. The initial condition over the 2-D domain

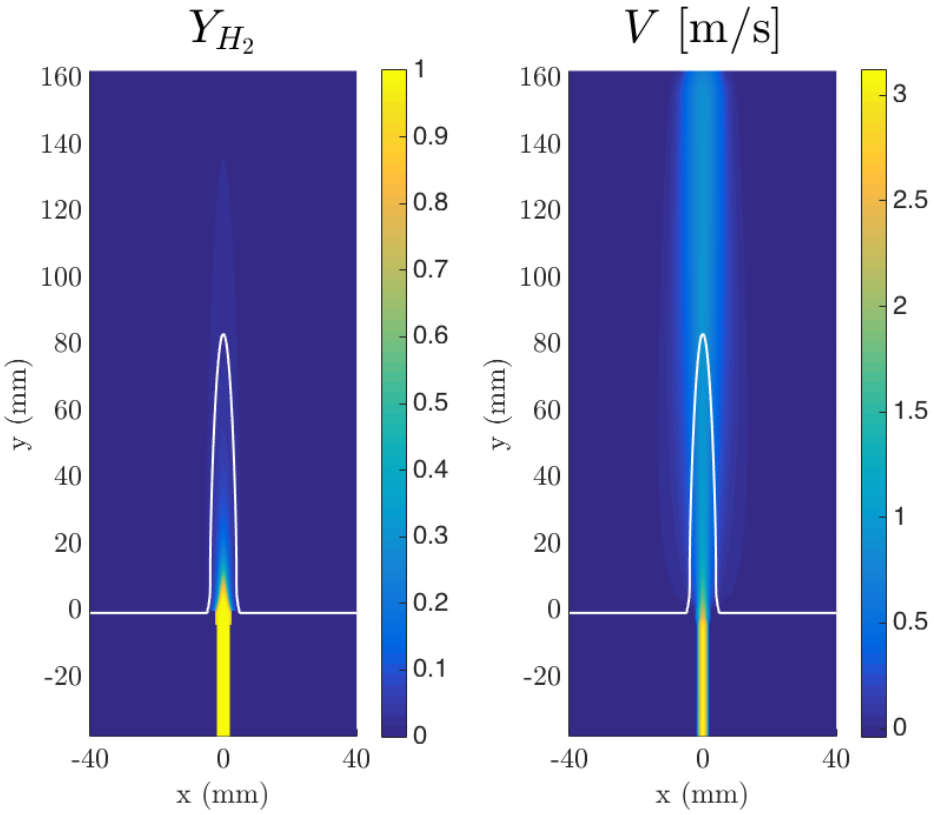

Figure 1: 2-D axisymmetric computational domain for the ignition case. Left: H_2 mass fraction at $t = 0$. Right: flow y velocity at $t = 0$.

is a stabilized cold hydrogen fuel jet (about 3 m/s) into a squared domain filled with air. The Fig. 1 illustrates this initial flow by showing the H_2 mass fraction and y-velocity.

Let

$$\boldsymbol{\zeta} = (\ln(A_3), b_3, \ln(E_3), L_{TW}, R_{TW}, M_e, E_{abs})^T$$

represent the random vector of uncertain model parameters, and $Q(\mathbf{x}, t; \boldsymbol{\zeta})$ be a quantity related to the solution of combustion system, and $Q_0(\mathbf{x})$ is its initial value. We can define the following quantity that links the mass fraction of fuel H_2 and oxidizer O_2 for the reaction (9),

$$\Phi(\mathbf{x}, t; \boldsymbol{\zeta}) = \frac{\nu'_{H_2,3} Y_{O_2}/W_{O_2}}{\nu'_{O_2,3} Y_{H_2}/W_{H_2}} = \frac{Y_{O_2}}{8 Y_{H_2}}.$$

Thus, the contour

$$\Phi(\mathbf{x}, t; \boldsymbol{\zeta}) = 1$$

defines the stoichiometric surface. E.g. the white contour in Fig. 1 represents the (stabilized) initial stoichiometric surface.

A spatial weighting function $w(\mathbf{x}, t; \boldsymbol{\zeta})$ can be defined following a Gaussian pdf with

respect to Φ,*

$$w(\mathbf{x}, t; \boldsymbol{\zeta}) = \frac{1}{\sigma\sqrt{2\pi}} \exp\left(-\frac{(\Phi - 1)^2}{2\sigma^2}\right),$$

where σ is a predefined deviation parameter; we use $\sigma = 0.001$ in this work. The spatial integral of weighting function is denoted by

$$\Omega(t; \boldsymbol{\zeta}) = \int w(\mathbf{x}, t; \boldsymbol{\zeta})\, \mathrm{d}\mathbf{x}.$$

The QoI used in this work is defined as a dimensionless average as follows

$$\mathcal{J}_Q(t; \boldsymbol{\zeta}) = \frac{\frac{1}{\Omega(t;\boldsymbol{\zeta})} \int Q(\mathbf{x}, t; \boldsymbol{\zeta}) w(\mathbf{x}, t; \boldsymbol{\zeta})\, \mathrm{d}\mathbf{x}}{\frac{1}{\Omega_0} \int Q_0(\mathbf{x}) w_0(\mathbf{x})\, \mathrm{d}\mathbf{x}} = \frac{\langle Q(t; \boldsymbol{\zeta}) \rangle}{\langle Q_0 \rangle}.$$

If $\mathcal{J}_Q(t \gg t_0; \boldsymbol{\zeta})$ is close to unity for a quantity such as temperature, it is obvious no ignition has appeared. Fig. 2 illustrates the temperature field of an ignited example, in which case the stoichiometric surface is heated by combustion and thus we have a high $\mathcal{J}_T$.

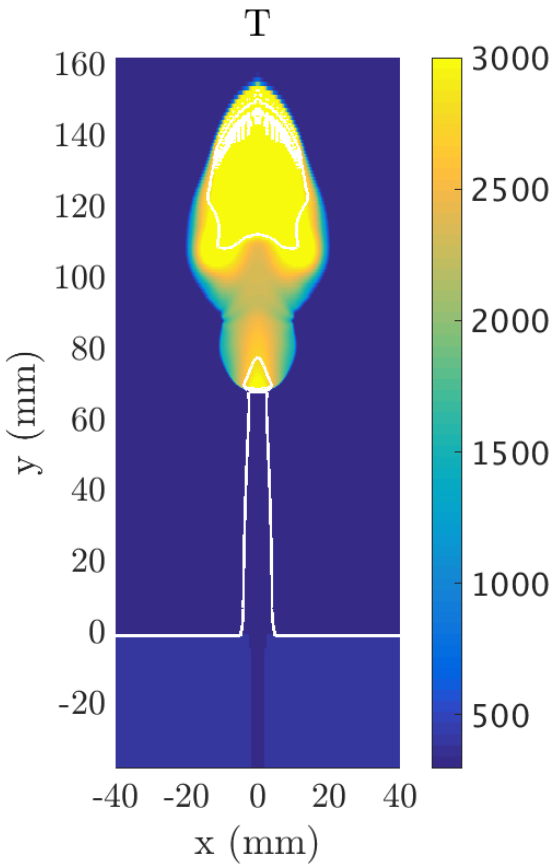

Figure 2: A successful ignition example. Compuational domain with a typical temperature field in [K]. Laser height: $y = 103.40$ mm.

*In present case where the stoichiometric surface under flame prpopagation does not change its form significantly in time, we can use a time-independent weighting function $w_0(\mathbf{x})$ for simplicity.

3.3 Uncertainty propagation and analysis

This section is devoted to the parameter sensitivity analysis for QoI $\mathcal{J}_T$. Let us analyze the case where the laser source is put at height $y = 103.40$ mm (with respect to experiments). We set the ANOVA interaction order $\nu = 3$ and size of experimental design $\mathcal{Q} = 100$.

The scatter plots of QoI with respect to each (tranformed) parameter are given in Fig. 3. Note here we employ the following isoprobabilistic tranform by using the cumulative distribution function (CDF) $\mathcal{F}$,

$$\xi_i = \mathcal{F}_{\zeta_i}(\zeta_i).$$

By definition $\mathcal{J}_T$ represents the dimensionless average temperature weighted on the initial-time stoichiometric surface. If we assume the raise of flame temperature in the vicinity of stoichiometric surface is mainly due to the release of enthalpy of formation of chemical reaction itself (not due to laser heat transfer), it is obvious that the greater the value of $\mathcal{J}_T$, the faster the flame propagates. Thus from Fig. 3 and as expected, we observe qualitatively

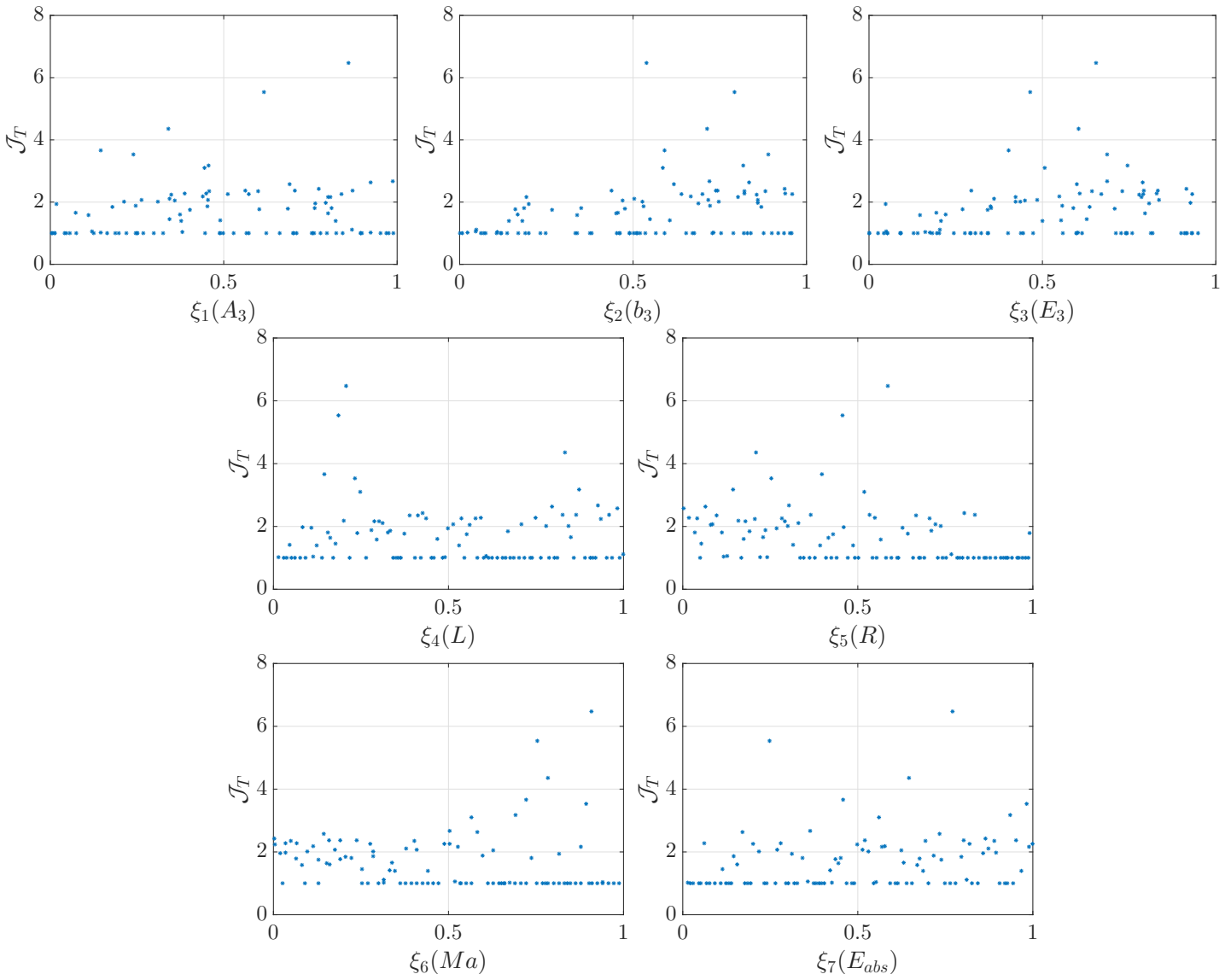

Figure 3: QoI vs. model parameters. Laser height: $y = 103.40$ mm.

with a stronger laser source (greater E_{abs} or smaller R_{TW} i.e. a more narrow region of high temperature), the more probably ignition occurs, and if this happens, the faster flame propagates. Also, a greater value of Mach number parameter M_e makes ignition more diffcult to happen because of the flow mixing; however, once ignited the flame is found to propagate considerably faster due to the vorticity. Concerning the remaining model parameters, we find it more difficult to draw a similar qualitative conclusion.

A procedure of parameter re-ordering is generally required (see end of Section 2) that depends upon their variance contribution of first-order ANOVA components.[†] Fig. 4 (top) presents the SI of input parameters, while the bottom figures illustrate the SI in the descending order together with the cumulated value. We denote the re-ordered input random vector for case $m = 4$ as,

$$\hat{\boldsymbol{\xi}}_{m=4} = (\xi_3, \xi_2, \xi_4, \xi_5, \xi_1, \xi_7, \xi_6)^T, \tag{10}$$

and for $m = 5$,

$$\hat{\boldsymbol{\xi}}_{m=5} = (\xi_2, \xi_3, \xi_4, \xi_5, \xi_1, \xi_7, \xi_6)^T. \tag{11}$$

Note they are slightly different about the relative importance of b_3 and E_3. In fact, the SI of b_3 and E_3 are very close in the case of $m = 5$.

Active dimension D_2 is evaluated using the sum of variances of first-order terms

$$\sum_{i=1}^{D_2} \mathrm{Var}(f_i) \geqslant p \sum_{i=1}^{N} \mathrm{Var}(f_i), \tag{12}$$

where p is a proportionality constant in $(0, 1)$, and is very close to 1. Thus we can conclude from Fig. 4 the following

$$\begin{aligned} D_2 &= 3, \quad \text{if } p = 0.7, \\ D_2 &= 4, \quad \text{if } p = 0.8, \\ D_2 &= 5, \quad \text{if } p = 0.9, \\ D_2 &= 6, \quad \text{if } p = 0.95, \\ D_2 &= 7, \quad \text{if } p = 0.999. \end{aligned}$$

We set $p = 0.999$ for this case, which results that all input parameters are taken into consideration for interaction calculations. In fact, the dimensionality of 7 is relatively low, and the proposed adaptive approach can handle this problem with an experimental design size $\mathcal{Q} = 100$ by setting this high active dimensionality at this stage. As a result, the ANOVA expansion has its size equal to

$$N + \binom{D_2}{2} + \binom{D_3}{3} = 63.$$

Fig. 5 illustrates the first-order SI together with total sensitivity indices (TSI). We observe that the kinetic parameters have a more significant variance contribution than their laser source counterparts in general. Meanwhile, both measures indicate the input parameter $\xi_3(E_3)$ is the most significant one, followed by $\xi_2(b_3)$. The TSI when setting $m = 5$ shows the variance contribution of the input $\xi_1(A_3)$ is more significant than all laser source parameters.

[†]We remind that this step involves a least-squares regression system that only contains polynomial bases of first-order.

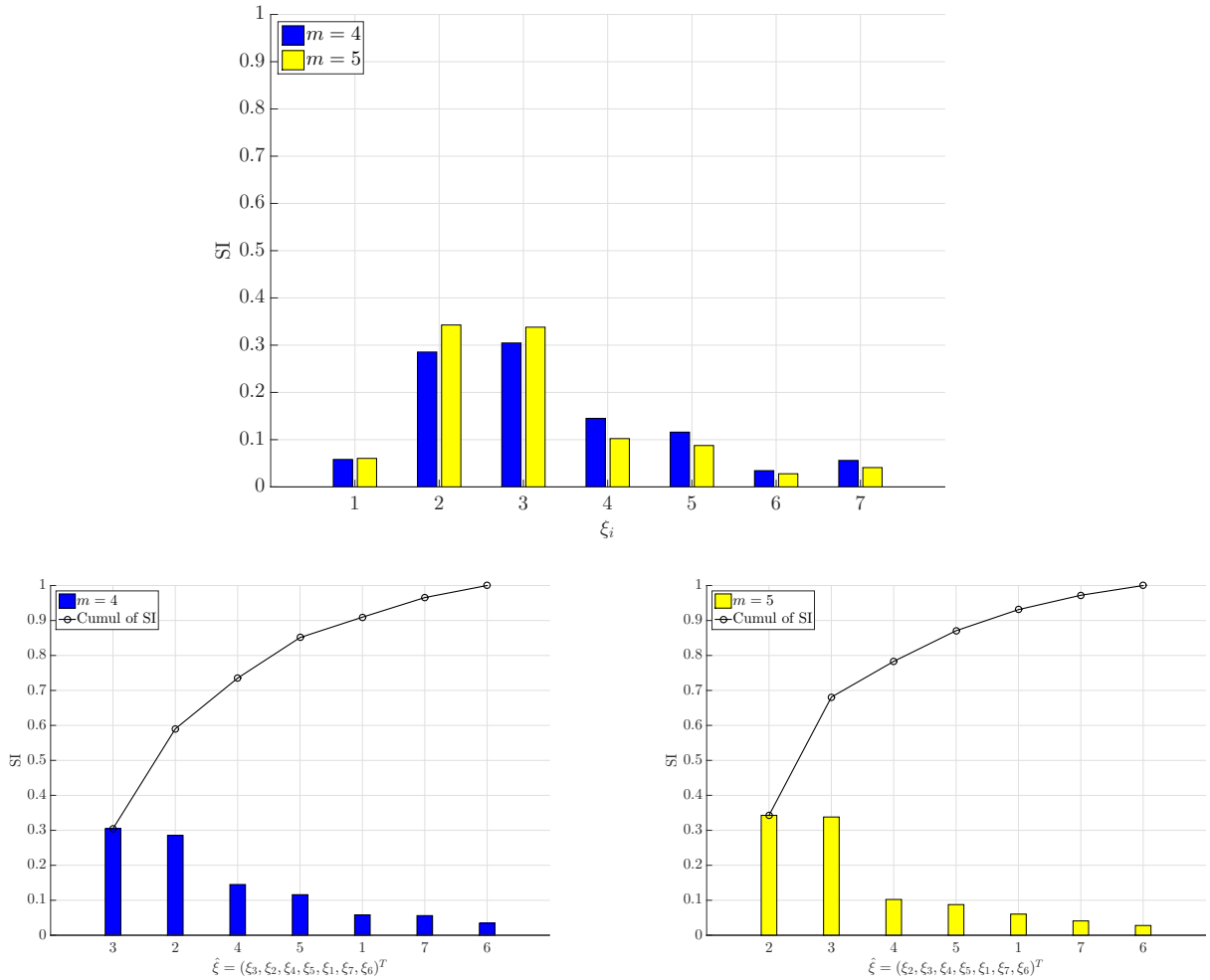

Figure 4: First-order SI for $m = 4$ and $m = 5$. x-axis indexing on the top figure is according to original random vector $\boldsymbol{\xi}$. $\hat{\boldsymbol{\xi}}$ on the bottom figures is the re-ordered input vector. $\nu = 3$. Experimental design size $\mathcal{Q} = 100$. $p = 0.999$. Laser height: $y = 103.40$ mm.

Fig. 6 illustrates the Sobol' sensitivity indices for both first- and higher-order ANOVA component functions. For the sake of clarity, we point out explicitly the following:

- $x-$axis indices $1-7$ represent first-order ANOVA components that are ordered according to the original random vector

$$\boldsymbol{\xi} \rightarrow \boldsymbol{\zeta} = (\ln(A_3), b_3, \ln(E_3), L_{TW}, R_{TW}, M_e, E_{abs})^T.$$

- $x-$axis indices $8-28$ represent second-order ANOVA components, while $29-63$ represent third-order ones. These indices are ordered following $\hat{\boldsymbol{\xi}}$ (10) or (11), and by using an ANOVA multi-index system presented in [19, page 1556].

We then mostly observe from Fig. 6 that the interaction between b_3 and $\ln(E_3)$ is significant compared to first-order and other interaction contributions. The third-order interactions are in general of less importance than second- and first-order components.

4 CONCLUSIONS AND FUTURE WORK

This paper aims to deal with Uncertainty Quantification of engineering and physical problems featuring a moderate to large number of uncertain input parameters. The purpose is to identify the relative importance of these uncertainties onto a given quantity of interest. This is achieved in this work by performing global sensitivity analysis, and in particular by combining the Analysis of Variance technique (ANOVA) and the polynomial dimensional decomposition approach (PDD). A set of coupled adaptivity strategies are futher employed and have been proved useful to identify important parameters in a simplified plasma-assisted combustion system.

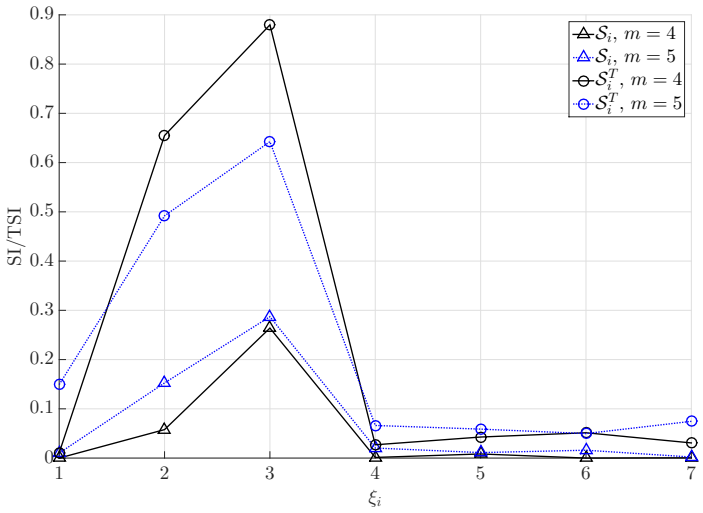

Figure 5: First-order Sobol' Sensitivity Indices (SI) and Total Sensitivity Indices (TSI). $\nu = 3$. $m = 4, 5$. Experimental design size $\mathcal{Q} = 100$. $p = 0.999$. All 7 parameters are considered in first- and higher-order ANOVA components. Laser height: $y = 103.40$ mm.

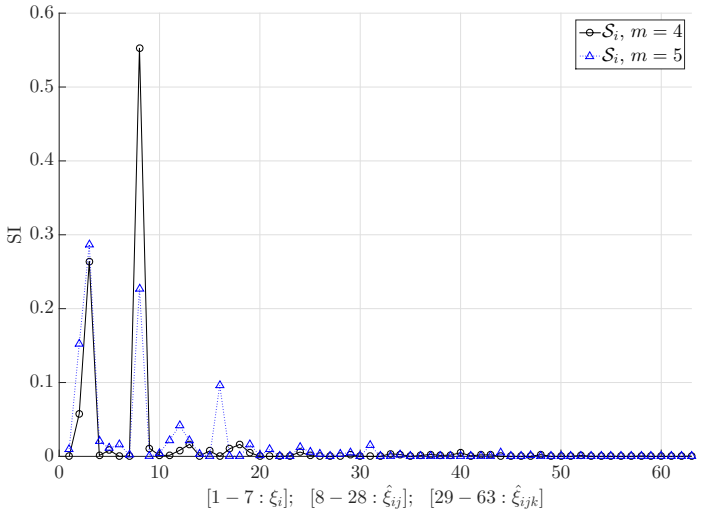

Figure 6: First-, second- and third-order Sobol' Sensitivity Indices (SI). The element indices of the original input vector $\boldsymbol{\xi}$ are used for first-order SI, while the ones of the re-ordered input vector $\hat{\boldsymbol{\xi}}$ are used for second- and third-order SI. $\nu = 3$. $m = 4, 5$. Experimental design size $\mathcal{Q} = 100$. $p = 0.999$. All 7 parameters are considered in first- and higher-order ANOVA components. Laser height: $y = 103.40$ mm.

The resulting surrogate polynomial approximation is a very sparse representation of the deterministic model. Since the surrogate model size is updated recursively in the stepwise regression procedure, the number of the required deterministic model evaluations is well controlled, and its final value is significantly smaller than when employing a standard Monte Carlo or quasi Monte Carlo method. Finally, the computation of the global sensitivity indices simply requires a post-processing of the polynomial coefficients.

More detailed models for Laser Induced Breakdown and Laser-Plasma Interaction are currently in development in XPACC, while we are also considering more detailed chemistry mechanism for future work. A dielectric-barrier discharge (DBD) force and radical generation model will also be included in our future parametric UQ study.

ACKNOWLEDGMENT

This material is based in part upon work supported by the Department of Energy, National Nuclear Security Administration, under Award Number DE-NA0002374.

References

[1] G. E. B. Archer, A. Saltelli, and I. M. Sobol'. Sensitivity measures, anova-like techniques and the use of bootstrap. *Journal of Statistical Computation and Simulation*, 58:99–120, 1997.

[2] Philip S. Beran, Chris L. Pettit, and Daniel R. Millman. Uncertainty quantification of limit-cycle oscillations. *Journal of Computational Physics*, 217(1):217–247, 2006.

[3] G. Blatman and B. Sudret. Efficient computation of global sensitivity indices using sparse polynomial chaos expansions. *Reliability Engineering and System Safety*, 95:1216–1229, 2010.

[4] Géraud Blatman and Bruno Sudret. An adaptive algorithm to build up sparse polynomial chaos expansions for stochastic finite element analysis. *Probabilistic Engineering Mechanics*, 25(2):183–197, April 2010.

[5] Géraud Blatman and Bruno Sudret. Adaptive sparse polynomial chaos expansion based on least angle regression. *Journal of Computational Physics*, 230(6):2345–2367, March 2011.

[6] E Borgonovo, G E Apostolakis, S Tarantola, and A Saltelli. Comparison of global sensitivity analysis techniques and importance measures in PSA. *Reliability Engineering & System Safety*, 79(2):175–185, 2003.

[7] Seung-Kyum Choi, Ramana V. Grandhi, Robert A. Canfield, and Chris L. Pettit. Polynomial Chaos Expansion with Latin Hypercube Sampling for Estimating Response Variability. *AIAA Journal*, 42(6):1191–1198, 2004.

[8] Toshimitsu Homma and Andrea Saltelli. Importance measures in global sensitivity analysis of nonlinear models. *Reliability Engineering & System Safety*, 52(1):1–17, 1996.

[9] O. Le Maître, M. T. Reagan, H. N. Najm, R. G. Ghanem, and O. M. Knio. A Stochastic Projection Method for Fluid Flow II. Random Process. *Journal of Computational Physics*, 181(1):9–44, September 2002.

[10] Luca L. Massa and Jonathan B Freund. An Integrated Predictive Simulation Model for the Plasma-Assisted Ignition of a Fuel Jet in a Turbulent Crossflow. In *54th AIAA Aerospace Sciences Meeting*, number January, pages 1–48, Reston, Virginia, jan 2016. American Institute of Aeronautics and Astronautics.

[11] Hermann G. Matthies and Andreas Keese. Galerkin methods for linear and nonlinear elliptic stochastic partial differential equations. *Computer Methods in Applied Mechanics and Engineering*, 194(12-16):1295–1331, 2005.

[12] Sharif Rahman. A polynomial dimensional decomposition for stochastic computing. *International Journal for Numerical Methods in Engineering*, 76:2091–2116, 2008.

[13] Sharif Rahman. Global sensitivity analysis by polynomial dimensional decomposition. *Reliability Engineering & System Safety*, 96(7):825–837, July 2011.

[14] Sharif Rahman and Xuchun Ren. Novel computational methods for high-dimensional stochastic sensitivity analysis. *International Journal for Numerical Methods in Engineering*, 2014.

[15] Sharif Rahman and Vaibhav Yadav. Orthogonal Polynomial Expansions for Solving Random Eigenvalue Problems. *International Journal for Uncertainty Quantification*, 1(2):163–187, 2011.

[16] I. M. Sobol'. Sensitivity estimates for nonlinear mathematical models. *Mathematical Modelling & Computational Experiments*, 1(4):407–414, 1993.

[17] I. M. Sobol'. Global sensitivity indices for nonlinear mathematical models and their Monte Carlo estimates. *Mathematics and Computers in Simulation*, 55(1-3):271–280, February 2001.

[18] B. Sudret. Global sensitivity analysis using polynomial chaos expansions. *Reliability Engineering & System Safety*, 93(7):964–979, July 2008.

[19] Kunkun Tang, Pietro M. Congedo, and Rémi Abgrall. Sensitivity analysis using anchored ANOVA expansion and high-order moments computation. *International Journal for Numerical Methods in Engineering*, 102(9):1554–1584, June 2015.

[20] Kunkun Tang, Pietro M. Congedo, and Rémi Abgrall. Adaptive surrogate modeling by ANOVA and sparse polynomial dimensional decomposition for global sensitivity analysis in fluid simulation. *Journal of Computational Physics*, 314:557–589, jun 2016.

[21] Vaibhav Yadav and Sharif Rahman. Adaptive-sparse polynomial dimensional decomposition methods for high-dimensional stochastic computing. *Computer Methods in Applied Mechanics and Engineering*, 274:56–83, June 2014.